Master's Thesis

PKR Phosphorylation as an Indicator for Echovirus 1 Genome Egress from Endosomes

William Aspelin

University of Jyväskylä

Department of Biological and Environmental Science

Cell and Molecular Biology

10 November 2019

UNIVERSITY OF JYVÄSKYLÄ, Faculty of Mathematics and Science
Department of Biological and Environmental Science
Cell and Molecular Biology

William Aspelin: PKR Phosphorylation as an Indicator for Echovirus 1 Genome Egress from Endosomes
MSc thesis: 40 p., 1 appendix (1 p.)
Supervisors: MSc Mira Laajala and PhD Varpu Marjomäki
Reviewers: PhD Jonna Nykky ja PhD Jessica Rumfeldt

November 2019

Keywords: eIF2, infection, kinase, oligonucleotide, stress, timeline, translation

Pathogens may trigger various antiviral responses in eukaryotic cells. One such response is preventing viral translation by eukaryotic initiation factor 2 (eIF2) phosphorylation. Protein kinase double-stranded RNA-dependent (PKR) is an eIF2 kinase activated by phosphorylation after exposure to double-stranded RNA (dsRNA). Though they act as hub elements for several stress signalling pathways, PKR and eIF2 phosphorylation is strongly associated with antiviral responses. Echovirus 1 (EV1) belongs to the enterovirus subgroup B, many members of which have been implicated in the development of type 1 diabetes in individuals exposed to the virus as infants, sparking interest in their biology and the development of drugs and vaccines. The major entry route of EV1 is via endosomal-like vesicles in which the uncoating of the genome occurs. How and when echoviral genomes cross this membrane barrier to the cytoplasm is not well known. Here we demonstrate that the phosphorylation of PKR can be induced by dsRNA composed of released EV1 genomes and transfected oligonucleotide probes. Furthermore, this phosphorylation can be detected by Western blot and used to demonstrate that echovirus 1 genomes cross the endosomal membrane barrier approximately 2.5−3.5 hours post-infection in A549 cells. If developed further, this new method may help characterise the mechanism of endosomal egress and any proteins involved as well as provide a tool for anti-echoviral drug and vaccine development.

JYVÄSKYLÄN YLIOPISTO, Matemaattis-luonnontieteellinen tiedekunta
Bio- ja ympäristötieteiden laitos
Solu- ja molekyylibiologia

William Aspelin: PKR:n fosforylaatio echovirus 1:n genomin endosomista vapautumisen indikaattorina
Pro gradu -tutkielma: 40 s., 1 liite (1 s.)
Työn ohjaajat: MSc Mira Laajala ja Tri. Varpu Marjomäki
Tarkastajat: Tri Jonna Nykky ja Tri. Jessica Rumfeldt
Marraskuu 2019

Hakusanat: aikajana, eIF2, infektio, kinaasi, oligonukleotidi, stressi, translaatio

Isäntäsolut ovat kehittäneet useita keinoja tunnistaa viruksia ja estää niiden lisääntyminen. Yksi näistä keinoista on translaatioon vaadittavan tukiproteiini eukaryotic intiation factor 2:n (eIF2) fosforylaatio, joka estää translaation tehokkaasti. Kaksijuosteisesta RNA:a (dsRNA) aktivoituva protein kinase dsRNA-dependent-proteiini (PKR) on eIF2 kinaasi, joka itsefosforyloituu aktivoituessaan. Sekä PKR:N että eIF2:n fosforylaatio yhdistetään usein antiviraaliseen soluviestintään. Echovirus 1 (EV1) kuuluu enterovirusten B-alaryhmään, jonka jäsenistä useat on yhdistetty tyypin 1 diabeteksen puhkeamiseen sille altistuneissa lapsissa. Se tunkeutuu isäntäsoluihin endosominkaltaisissa rakkuloissa ja vapauttaa genominsa proteiinikuoresta näissä rakkuloissa. Ei ole täysin varmaa miten EV1 genomi pääsee rakkulakalvon läpi solulimaan, jossa translaatio ja replikaatio tapahtuvat. Tässä työssä osoitamme, että EV1-infektoituihin soluihin transfektoidut virusgenomille komplementaariset oligonukleotidikoettimet aktivoivat PKR:n fosforylaatiota muodostaessaan kompleksin virusgenomin kanssa solulimassa. Tätä fosforylaatiota voi käyttää osoittamaan, että EV1 genomi on vapautunut endosomirakkulasta solulimaan, mikä tapahtui A549 soluissa noin 2,5−3,5 tuntia infektion jälkeen. Pidemmälle kehitettynä tämä uusi metodi voi tulevaisuudessa auttaa selvittämään, miten EV1:n genomi vapautuu endosomista, löytämään siihen liittyviä proteiineja sekä kehittämään lääkkeitä ja rokotteita EV1:ä vastaan.

TABLE OF CONTENTS

TERMS AND ABBREVIATIONS

TERMS

Endosomal egress	The process of leaving the confines of an endosomal vesicle

ABBREVIATIONS

EV1	Echovirus 1
PKR	Protein kinase double-stranded RNA dependent
eIF2	Eukaryotic initiation factor 2
eIF2α	Alpha subunit of eukaryotic initiation factor 2
p.i.	post-infection

1 INTRODUCTION

1.1 Echovirus 1

Echovirus 1 (EV1), like all viruses in the genus enterovirus, is an icosahedral, single-stranded positive-sense RNA virus which belongs to the family Picornaviridae (Tuthill et al., 2010). Prominent hosts of enteroviruses include several species of mammals, including humans, in which primary sites of infection are the gastrointestinal tract, and the upper respiratory system. Enteroviral infections, especially those of primary tissue, may be symptomless or mild: when first isolated, EV1 was not associated with any disease. However, some enteroviruses have been observed to be capable of causing more severe symptoms or infecting secondary tissues with potentially devastating effects in the form of inflammatory diseases e.g. meningitis (Harley et al., 1998) or myocarditis (Roivanen et al., 1998). Moreover, the presence of neutralising antibodies against certain species, such as EV1, in the serum of infants has been associated with the development or exacerbations of other, more chronic conditions such as type I diabetes in infants (Laitinen et al., 2014). Due to these implications, there is an increasing interest in developing anti-enteroviral and anti-echoviral drugs and vaccines.

1.1.1 Genome and structure

EV1 is one of more than 30 serotypes in the species enterovirus B and is thought to share most of its general structural and genetic features with the type species of enterovirus, coxsackievirus B3, as well as poliovirus, one of the best-studied enteroviruses (Marjomäki et al., 2015). The 5′ end of the genome is covalently liked to a small viral protein (VPg) which acts as a protein primer for its viral RNA polymerase (Paul et al. 1998). The genome mimics eukaryotic mRNA with a polyadenylated 3′ end (Yogo and Wimmer, 1972). The actual coding region is

flanked by extensive untranslated regions designated 5′ and 3′ noncoding regions (Wimmer et al., 1993). The three-dimensional folding patterns of these regions are thought to contribute to translation regulation, replication, and packaging as certain mutations in these regions hinder these activities (Wimmer et al., 1993).

The icosahedral capsid consists of a total of 60 copies of three main structural proteins VP1, VP3, and VP0, the latter of which is cleaved into two separate entities, VP2 and VP4, during virus particle maturation associated with genome encapsidation (Tuthill et al., 2010). Underneath the main capsid protein VP1, within a canyon-like indentation in the capsid, is a hydrophobic pocket which contains a fatty acid (Filman et al., 1989), commonly referred to as a pocket factor. This lipid is ejected from the pocket during uncoating and is thought to stabilise the capsid, perhaps to the point of preventing uncoating if not removed (Smyth et al., 2003, Tuthill et al., 2010). These features make the hydrophobic pocket a promising target for future antiviral drug development.

1.1.2 Entry

The bulk of EV1 internalisation is thought to occur by a macropinocytic-like mechanism, though experimental data seems to suggest that the virus may use several entry routes (Marjomäki et al., 2015). The virus has been detected lodged in host cell calveolae and later-stage entry vesicles generally contain caveolin-1 (Marjomäki et al., 2002, Karjalainen et al., 2008). However, caveolar internalisation is unlikely to be a major entry route because early internalisation vesicles lack caveolar markers (Marjomäki et al., 2002, Karjalainen et al., 2008). Clathrin-independent endocytic route is thought to be the most common entry mechanism (Marjomäki et al., 2015). EV1 capsids have demonstrated extensive interactions with α2β1 integrin and the two colocalise during entry, making it a likely primary receptor (Bergelson et al., 1992, Xing et al., 2004).

Initial receptor binding occurs near glycosylphosphatidylinositol-anchored protein-rich lipid rafts after which α2β1 integrin starts to accumulate at the site (Pietiäinen et al., 2004). This accumulation triggers the internalisation of both receptors and viral particles in tubular vesicle structures (Pietiäinen et al., 2004, Karjalainen et al., 2008). These entry vesicles develop into intraluminal vesicle-rich multivesicular bodies, which begin to accumulate caveolin-1 and possibly assimilate various caveosomes and their contents into their mass (Marjomäki et al., 2002, Karjalainen et al., 2008). Unlike the proposed entry routes of many picornaviruses, these multivesicular bodies induced by EV1 infection seem to be separate from the normal α2β1 integrin-recycling endosomal pathway, and do not acidify (Karjalainen et al., 2011, Rintanen et al., 2012).

1.1.3 Uncoating and endosomal egress

EV1 uncoating events are pH-independent and require the formation of these atypical endosomal vesicles for successful capsid destabilisation (Karjalainen et al., 2011). According to the current model, EV1 destabilisation and uncoating involves structural changes which occur in stages to allow RNA release from an open capsid, canonically referred to as an altered particle. This particle is characterised by openings at 2-fold symmetry axes, the expulsion of pocket factors, externalisation of VP1 N-termini, and the release of VP4 from the particle (Bostina et al., 2011, Butan et al., 2014, Myllynen et al., 2016). Myllynen et al. (2016) describe a more open and porous form of the capsid which could be a semi-stable intermediate between a fully open particle and an intact one. These changes could be triggered by receptor interactions and, consequently, make the rest of the uncoating cascade possible.

How EV1 genomes escape the confines of these endosomal vesicles is not yet clear. One of the likely candidates is a membrane-rupturing or pore-forming mechanism. Such intracellular pathogenic microbes as *Mycobacterium tuberculosis* and *Shigella flexneri* have been observed to utilise somewhat radical methods to rupture

membranes of infected cells (Keller et al., 2013). These tears in cell membrane can be so extreme that they are cytotoxic, even leading to apoptosis or necrosis (Simeone et al., 2012). However, such virulent effects have not been observed during EV1 infection, implying that the virus has evolved a subtler mechanism. Human rhinoviruses, close relatives of EV1, are known to form small, size-selective pores on membranes with their VP4 proteins released during disassembly (Panjwani et al., 2014). Considering the close relation to EV1 combined with similarities in particle uncoating, including VP4 release, makes a similar mechanism of membrane poration very likely.

The exact time of endosomal egress is not yet certain. However, if uncoating events are not blocked within ca. 30 min post-infection (p.i.), ca. 5% of SAOS-α2β1 (Human osteosarcoma cells overexpressing α2β1-integrin) cells are infected by EV1 (Siljamäki et al., 2013). The portion of infected cells increases to normal levels of 20—30% if uncoating is prevented 1 hour p.i. or later. This could indicate that the majority of uncoating events occur ca. 30 minutes to an hour after infection. Permeability studies of EV1 infection in SAOS-α2β1 cells revealed that the integrity of EV1 infection-associated multivesicular bodies decreased from 1 to 3 hours p.i.: an increase in permeability correlated with increasing size and structural complexity of both multivesicular bodies and their intraluminal vesicles (Soonsawad et al., 2014). Significant amounts of both positive strand genomic RNA and complementary negative strands can be detected in the cytoplasm approximately 3 hours p.i. (Upla et al., 2008). Both positive and negative-sense RNA are signs of active replication and translation which are thought to occur soon after the genome enters the cytoplasm.

1.1.4 Translation, replication, and release

Once EV1 genomes reach the cytoplasm, translation may begin. The 5′ noncoding region contains an internal ribosome entry site element (Jang et al., 1990, Wimmer

et al., 1993). This internal ribosome entry site, together with the structures of the noncoding regions, allows host translation factors and ribosomal subunits to assemble in the middle of a nucleic acid stand in a cap-independent manner (Jang et al., 1990).

Viral translation occurs in the form of a single polyprotein and it is later processed by self-cleaving motifs in the polyprotein itself (Palmenberg 1990). Initial cleavages of the polyprotein produce three main precursor products which, based on the functions of progeny proteins, can be roughly divided into structural P1, and non-structural P2 and P3. Non-structural proteins include an RNA-polymerase, constituents of the replication machinery, and peptides that modify host responses and processes.

The infection cycle advances from active translation to replication through a molecular switch mechanism thought to involve viral protease 3C(pro) (Back et al., 2002). By cleaving various host proteins, 3C(pro) produces peptides that inhibit Internal ribosome entry site-dependent translation, allowing RNA synthesis to take over (Back et al., 2002). Assisted by various non-structural viral proteins, the viral RNA polymerase $3D^{pol}$ produces a negative-sense genome (Flanegan and Baltimore, 1977, Paul et al., 1998). The few negative-sense strands are then used by the same viral polymerase as templates for the mass production of positive-sense genomes for packaging (Flanegan and Baltimore, 1977).

Like many positive-sense RNA viruses, the replication of enteroviruses, such as EV1, induces host membrane rearrangements (Belov et al., 2013 and Belov et al., 2014). Viral proteins alter the function of membrane remodelling proteins to create tubular, lobar, and vesicular structures (Hsu et al., 2010, Ilnytska et al., 2013). Replication complexes strongly associate with these altered membranes throughout the infection (Belov et al., 2014). These structures are sometimes referred to as replication organelles, as they are vital to replication *in vivo* and may contribute to

non-lytic secretion of viral particles (Hsu et al., 2010, Belov et al., 2014, and Chen et al., 2015).

Though the exact mechanism of enterovirus assembly is poorly understood, it is known that the viral structural proteins VP1, VP3, and VP0 self-assemble into pentamers in the cytoplasm (Basavappa et al., 1994). They then aggregate around the viral genome forming a provirion. The presence of viral RNA then mediates particle maturation by inducing the cleavage of VP0 into two peptides VP2 and VP4 (Basavappa et al., 1994). These mature particles are then most likely released via cytolysis, though there is evidence of non-lytic pathways (Robinson et al., 2014).

1.2 Antiviral roles of eIF2 and PKR

Viruses and their host cells are engaged in a perpetual arms race: in the course of their evolution, viruses have developed ways to exploit their hosts' weaknesses in order to replicate at their expense. In turn, susceptible cells have evolved to recognise and repel invading pathogens. When triggered, antiviral pathways can result in various changes in host metabolism, collectively known as "antiviral states". Non-native RNA or DNA structures are some of the strongest indicators of a virus infection and are the target pathogen-associated molecular pattern of many toll-like receptors and interferons (reviewed by Takeuchi and Akira, 2009).

1.2.1 Eukaryotic initiation factor 2 phosphorylation

Eukaryotic initiation factors, or eIFs, are eukaryotic proteinaceous elements associated with complexes required for the translation of mRNA (eukaryotic translation reviewed by Hinnebusch, 2014). This historical nomenclature spans several diverse and functionally different proteins which participate in the initiation and control of translation as well as post-translational processing of translation machinery in various ways. In eukaryotes, most translates begin with a methionine

residue which, pre-assimilation, is bound to a tRNA molecule. For this methionine-tRNA to initiate a translation event, it needs to form a complex with GTP-bound eukaryotic initiation factor 2 (eIF2) and a small ribosomal subunit. When this complex detects a free mRNA AUG codon, GTP-eIF2 is converted to GDP-eIF2, inducing certain conformational changes that force the initiation factors to disassociate. Now there is enough room for the large ribosomal subunit to bind and catalyse the formation of the rest of this nascent polypeptide.

As a protein, eIF2 is a heteromultimeric protein composed of three structurally different subunits designated α, β, and γ (Hershey, 1989). Comparisons between eIF2 γ subunit sequences across various species revealed a relatively high level of homology, indicating that this element evolved early in the history of eukaryotic species and, to this day, has a crucial role in the regulation of translation (Erickson et al., 1997). The α and β subunits contain several phosphorylation sites associated with stress and starvation responses (van den Heuvel et al., 1995). Gamma subunit is thought to contain guanosine-binding domains and is suspected to mediate interactions with mRNA, since mutations in this subunit are most likely to render these interactions impossible (Gaspar et al., 1994).

Most eukaryotic cells have developed numerous mechanisms to combat viral infection, one of the main approaches being the inhibition of viral translation. Since eIFs are vital to translational control, they are the logical tools of the trade for said preventive measures and are the likely targets of post-translational modification. Various cellular kinases are known to phosphorylate the α subunit of eIF2 at its Ser51 residue, an event which effectively halts most translation events in a eukaryotic cell (**Error! Reference source not found.** B and C) (Meurs et al., 1990, van de Heuvel et al., 1995). In this phosphorylated state, eIF2 has a high affinity for the guanine nucleotide exchange factor responsible for replenishing the GTP; effectively turning eIF2 into a competitive inhibitor that prevents both components from participating in translation initiation (Kimball, 1999). Due to the efficacy of this

antiviral mechanism, some viruses have even developed specific anti-eIF2 kinase peptides to combat it (Huynh et al., 2017).

1.2.2 PKR kinase function and phosphorylation

One of the most studied eIF2α kinases is PKR, or protein kinase double-stranded RNA-dependent, found in both the cytoplasm and nucleus (Meurs et al., 1990). This kinase is thought to respond to double-stranded RNA (dsRNA) elements associated with pathogenic viruses and to convey the information of this threat to eIF2 by phosphorylating it (Cole, 2007). It can be roughly divided into two main domains: one exhibits kinase activity, the other detects the presence of long strands of dsRNA (Meurs et al., 1990, Romano et al., 1998).

Evidence that PKR conformation switches between open (or more active) and closed (with less affinity for dsRNA) states suggests that this protein is highly autoregulated (Dey et al., 2005, Lemaire et al., 2006). The stability of these states may be partially dependent on autophosphorylation events that are linked to monomer dimerisation in the cytoplasm. In a mode-of-activation model, Dey et al. (2005) and Cole (2007) theorise that PKR exists in an equilibrium between open and closed states, any random phosphorylation events staying at a negligible level in idle cells (**Error! Reference source not found.** A). During a stress response, PKR monomers would bind dsRNA, promoting dimerization (**Error! Reference source not found.** A and B) (Dey et al. 2005, Cole 2007). Dey et al. (2005) and Cole (2007) hypothesise that newly formed inter-dimer interactions would be stabilised by autophosphorylation events, which in turn would favour the active "open" conformation, and therefore increase the incidence of eIF2α phosphorylation events (**Error! Reference source not found.** B and C).

Stabilisation of PKR may also be mediated by phosphorylation by components of other signalling pathways. Many kinases are known to target it, and several of these

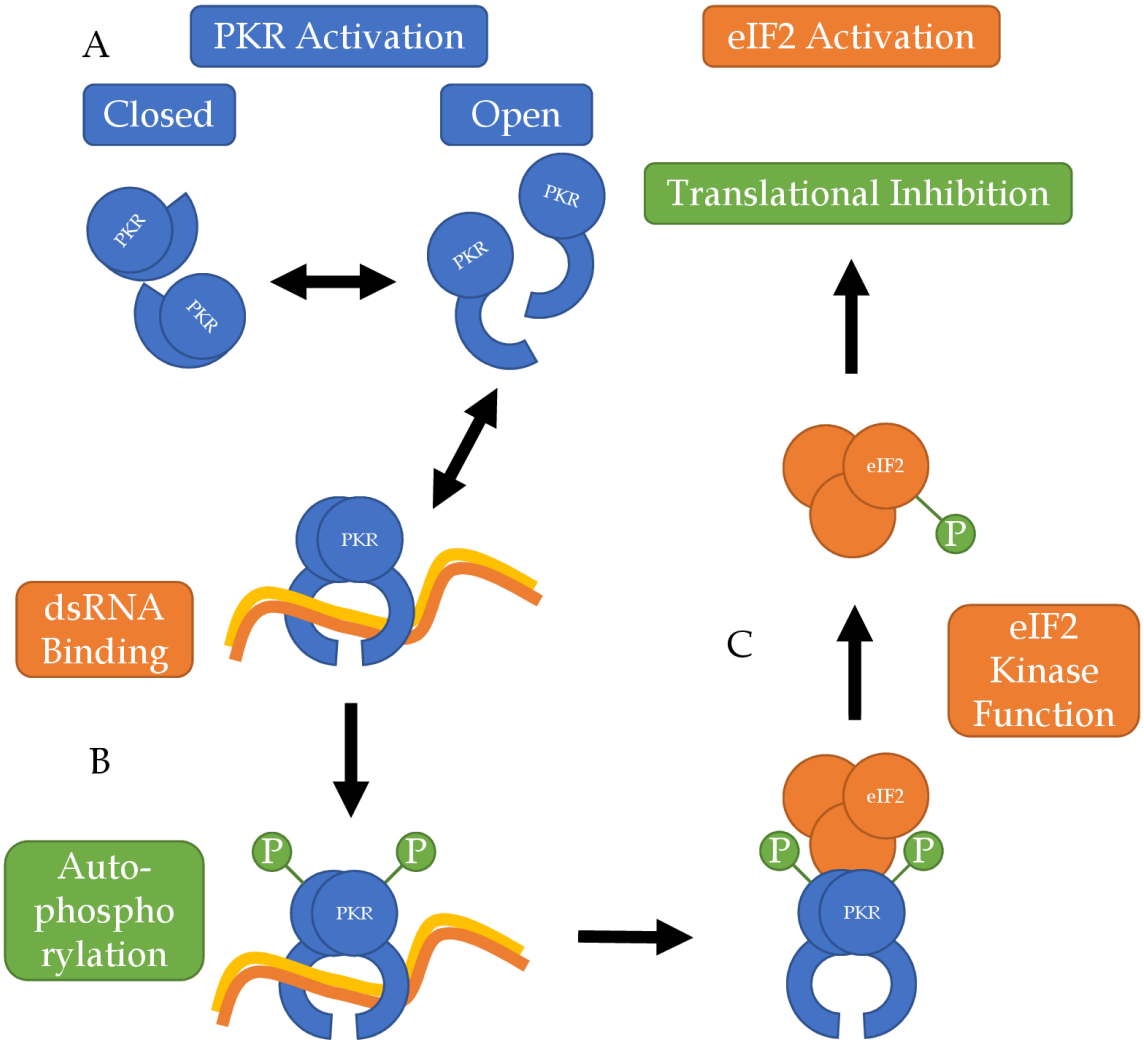

Figure 1. PKR and eIF2 activation. (A) PKR exists as an equilibrium between open and closed states. Interactions with dsRNA promote dimerisation. (B) Dimerisation is stabilised by autophosphorylation, activating the kinase domain. (C) eIF2 is activated by PKR when the alpha subunit is phosphorylated. This leads to translational inhibition.

processes have been characterised. However, most of them are thought to have minor effects on dimerisation, stability or RNA binding, and can be mutated without compromising kinase activity (Su et al., 2006). Conversely, preventing the autophosphorylation of threonine 446 completely abolishes PKR's eIF2α kinase function and has generally been associated with the activation of antiviral signalling (Dey et al., 1995, Romano et al., 1998). Therefore, Thr446 phosphorylation status

could potentially be used to monitor PKR status and the presence of dsRNA in the cytoplasm.

Although traditionally strongly associated with antiviral signalling in the presence of viral dsRNA, PKR may be activated by various other stress factors ranging from interferon signalling to amino acid starvation (Patel and Sen, 1998, Williams, 1999). The role of this kinase is further complicated by its promiscuity: several target proteins have been mapped and their effects are associated with a range of non-viral stress reactions. Notable targets include p53 (Cuddihy et al., 1999) and STAT family transcription factors (Deb et al., 2001, Lee et al., 2005).

The ultimate systemic cellular response to phosphorylation of eIF2 by PKR may vary drastically depending on currently unknown factors. Some studies report apoptotic signalling associated with eIF2α phosphorylation (Cuddihy et al., 1999, Scheuner et al., 2006) while others imply that it merely leads to a mild stress response or an antiviral state, promoting cell survival (Williams, 1999). Either response is consistent with the canonical ways in which cells combat viral infections and the ultimate fate of the cell may well depend on several other signalling states both upstream and downstream. PKR seems to be an intersection in the complex web of stress signalling where many pathways converge and diverge.

1.3 Aims of the study

PKR and eIF2 are phosphorylated at specific amino acids during a viral infection (Ser51 and Thr446, respectively). This study attempted to demonstrate that these phosphorylation events can be used to predict whether the genomes of EV1 have crossed the endosomal membrane barrier. Since dsRNA is highly prevalent in cells with actively replicating EV1, translation events (and therefore replication) were

halted with the drug cycloheximide. Cytoplasmic dsRNA was produced by transfecting oligonucleotide probe(s) complementary to the viral genome into infected cells. The formed duplexes of viral RNA and probe RNA induced PKR and eIF2 phosphorylation. Phosphorylated proteins were then detected with Western blot using phosphorylation-specific antibodies. The conditions necessary to detect these fluctuations in phosphorylation were to be explored and the protocols optimised.

The main research questions of this study were:

(1) Does the introduction of the probe(s) into infected cells induce PKR and eIF2 phosphorylation to a degree observable by Western blot so that one can conclude that endosomal egress has occurred?
(2) At what time post-infection do elevated rates of PKR and eIF2 phosphorylation suggest that viral genomes are generally released from endosomes?

It was hypothesised that these two proteins would be phosphorylated in the presence of viral genomes and the probe, and that the most phosphorylation would occur ca. 2−3 hours p.i., when the first signs of replication occur during normal infection.

As the mechanisms of enteroviral genome release and endosomal egress are not yet well understood, establishing a more accurate timeline for when the majority of these events occur in infected cells is vital to future studies on the topic. In addition to establishing such a timeline, it could potentially allow for the development of methods attempting to capture that moment of egress, and eventual characterisation of the processes and molecules involved. Furthermore, the ability to demonstrate whether or not endosomal egress has occurred has potential applications in many branches of virology research: such a method could be a new

tool in the characterisation of single-stranded RNA viruses, and be used to screen for antiviral drugs which affect endosomal egress or the steps before it.

2 MATERIALS AND METHODS

2.1 Cells and antibodies

The cells utilised in these experiments included doxycycline-inducible T7 polymerase-expressing Hela cells (courtesy of Giuseppe Balistreri, university of Helsinki) and A549 cells (Human lung epithelial carcinoma cells, ATCC catalogue CCL-185). The Hela cells were grown in constant 330 µg/ml geneticin and additionally in 1µg/ml doxycycline for four days prior to use in order to induce T7 polymerase expression when needed.

Cell culture was performed in complete Dulbecco's modified eagle medium (Gibco DMEM, Thermo Scientific): 10% foetal bovine serum (Gibco FBS, Thermo Scientific), 2mM L-glutamine (Gibco Glutamax, Thermo Scientific), 10 U/ml penicillin, and 10 µg/ml streptomycin (Gibco, Thermo Scientific).

Signalling events in the cell were monitored by using phosphorylation-specific antibodies: rabbit monoclonal anti-Phospho-Ser51-eIF2α (Cell Signalling Technology Inc.), and rabbit monoclonal anti-Phospho-T446-PKR (Abcam). Mouse polyclonal anti-actin (Sigma) was used as a reference standard and secondary horseradish peroxidase-recombinant goat anti-rabbit and goat anti-mouse antibodies were used for autoradiography detection (Cell Signalling Technology Inc.).

2.2 Oligonucleotide probes

Sequences complementary to the EV1 genome with recombinant T7 promoters (TAATACGACTCACTATAG) upstream from the sequence of interest were designed by Sami Oikarinen, University of Tampere. The most promising probes were used in the assay and titled T7p_E1F_1, T7p_E1F_2, and T7p_E1F_3

(Sequences in Appendix 1). These probes did not form homodimers and were not likely to form hairpin structures. Probes 2 and 3 had some minor homologies within the human genome, whereas probe 1 had none. DNA oligonucleotides of these sequences were synthesised by DNA dream Labs, University of Helsinki.

2.3 *In vitro* transcription

RNA probes were transcribed *in vitro* from the produced DNA probes using a Promega Riboprobe system T7 *In Vitro* Transcription kit, following kit instructions for large volume RNA transcription using 1.8 µg of template. The transcripts were purified by GE Healthcare ltd. Illustra Microspin G-50 columns and analysed by agarose gel electrophoresis. RNA concentration was determined spectroscopically (NanoDrop One UV-Vis Spectrometer, Thermo Scientific).

2.4 Transfection

Hela and A549 cells were transfected with both DNA and RNA probes using a lipid-based transfection kit (Lipofectamine 3000, Invitrogen). DNA probe concentration in the reaction mixture was either 20 or 100 nM. Approximately 500 ng of RNA was used when *in vitro* transcripts were used. In order to monitor T7 polymerase expression, an additional control transfected with 1 µg of pUC18 plasmid expressing mCherry under a T7 promoter (Courtesy of Tero Ahola, University of Helsinki) was prepared for DNA probe systems. Lipid-probe complex formation was performed in DMEM (Gibco DMEM, Thermo Scientific, no additives), which was then added into the medium of cells to be transfected for *ca.* 24 hours. Negative controls monitoring probe transfection background and the effect of transfection reagents were prepared when appropriate.

2.5 Infection

EV1 (Laboratory strain "Faroukh") infections of Hela and A549 cells were carried out on a 24-well plate in 300 µl of 100 mM cycloheximide in cold DMEM with (1% L-glutamine and 1% FBS) and the virus stock added into 50% confluent wells. Positive controls of EV1 infection without cycloheximide and negative controls of just 100 mM cycloheximide or plain medium were applied when necessary.

Virus stocks used were diluted 1:1000 in DNA probe assays (2.18 x 10^9 pfu per well) or 1:500 in RNA probe assays (4.36 x 10^9 pfu per well). Right after infection, the cells were incubated ranging from 15 minutes to 6 hours at 37 °C and 5% CO2, before lysis in 2X Laemmli buffer.

Lysate of Hela cells infected with semliki forest virus at 8 hours p.i., used as a positive control for eIF2 and PKR phosphorylation, was a kind gift from Giuseppe Balistreri lab, University of Helsinki.

2.6 Western blot

Samples were boiled in Laemmli buffer and loaded into the wells of a commercial precast SDS-PAGE gel (Mini protean TGX 4-20% Gels, Bio-Rad). The gel was run at 100 V for approximately 1−1.5 h and transferred onto a PVDF membrane (Immobilon-P, Merck) at 100 V for 1 h. The membranes were blocked with 5% bovine serum albumin (Bovine Serum Albumin, Sigma Life Sciences) in TBST before staining with primary antibodies diluted in 5% BSA in TBST. The membrane was then washed with TBST before further staining with secondary antibodies diluted in 5% BSA in TBST. After washing with TBST, the membranes were visualised by adding a horseradish peroxidase autoradiography reagent SuperSignal (SuperSignal West Pico Chemiluminescence Substrate, Thermo Scientific) and developed on radiographic film (Fujifilm SuperRX medical X-ray film).

2.7 Microscopy

Cells grown on coverslips were fixed with 4% paraformaldehyde for 30 min and treated with DAPI dye solution (Fischer Scientific, Molecular Probes DAPI). These cells were then mounted on objective glasses in Mowiol-DABCO mounting medium (Sigma-Aldrich) and imaged with fluorescent confocal microscopy (Olympus Fluoview 1000, helium-neon laser 543 nm channel and diode laser 405 nm channel, UPLFLN 40x oil immersion objective).

2.8 Statistical analysis

Western blot images (three for each condition analysed) were quantified by Fiji software (Schindelin *et al.* 2012) Gel Imaging plugin to give numerical values to band intensities referred to as a relative intensity. PKR and eIF2 phosphorylation values were normalised by comparing it with actin expression, quantified similarly. Using Excel (Microsoft Office, version 18.1903.1152.0), these values were then subjected to an unpaired two-tailed Welch's t-test because the two populations compared in each dataset were independent and expected to have different variations. The underlying assumption was that the null hypothesis could be rejected if mean phosphorylation of PKR/eIF2 (normalised with actin expression) increased significantly in the treated population as compared to the probe control population.

3 RESULTS

The main aim of this thesis was to develop and optimise an assay in which complementary probes against EV1 genome would produce a dsRNA structure the formation of which could be further detected via eIF2α and PKR phosphorylation. These events were detected by Western blot and phosphorylation status-specific antibodies. PKR is known to be actively phosphorylated in the presence of dsRNA, leading to its activation. Furthermore, active PKR phosphorylates eIF2α-subunits leading to the inhibition of protein translation in infected host cells. The phosphorylation of eIF2α and PKR was hypothesised to correlate with the endosomal egress of EV1 genome. The dsRNA structures detected were thought to mostly originate from EV1 genome and probe pairings as the formation of naturally occurring viral dsRNA structures during infection were prevented using cycloheximide

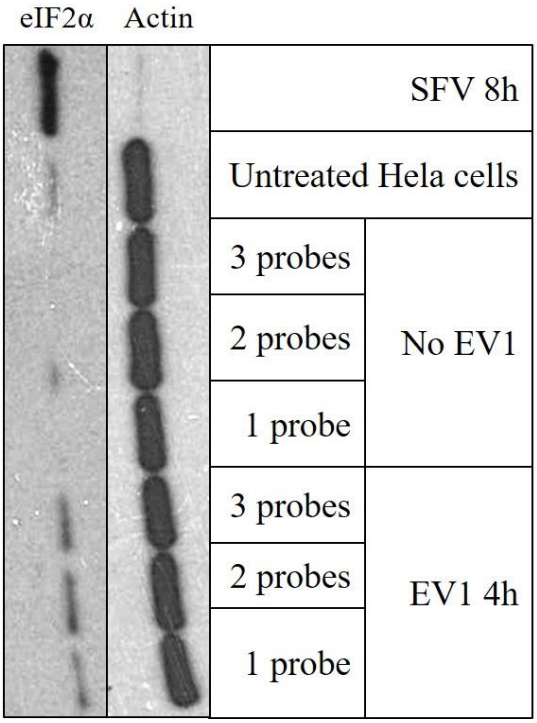

Figure 2. Phosphorylation of eIF2α in DNA probe-transfected and EV1-infected T7-Hela cells. Transfection with either just probe 1, probes 1 and 2, or all three were performed. The cells were lysed for Western blot 4 hours p.i. and stained with eIF2α phosphorylation- and actin-specific antibodies. Positive semliki forest virus (SFV) control confirmed that eIF2α phosphorylation could be detected with the antibody.

3.1 DNA probe transfection increases eIF2α phosphorylation

In subsequent experiments, RNA oligonucleotides complementary to viral RNA were produced by introducing DNA oligonucleotide probes, consisting of a T7 promoter and a homology sequence (full

sequences in Appendix 1), into T7 polymerase-expressing cells. Three different probes were selected: one with no major homology with the human genome and two additional ones with some potential off-targets. Initial tests were conducted by transfecting these probes into T7 polymerase-expressing Hela cells.

Semliki forest virus infected cell lysate (8 hours p.i.) was used as a control for eIF2α phosphorylation. Hela cells transfected by one, two or three probes indicated some increase in eIF2α phosphorylation (Figure 2) at 4 hours p.i.: higher levels of eIF2α phosphorylation in infected cells than in noninfected controls suggested that dsRNA composed of viral genomes and introduced probe(s) contributes to the increase in phosphorylation. The number of different probes transfected simultaneously did not affect phosphorylation levels observed. However, confocal fluorescent microscopy of fixed T7 Hela cells transfected with T7-mCherry suggested that the level of T7 polymerase activity was very low in these cells since only few expressed mCherry at high enough levels to be detected (Figure 3).

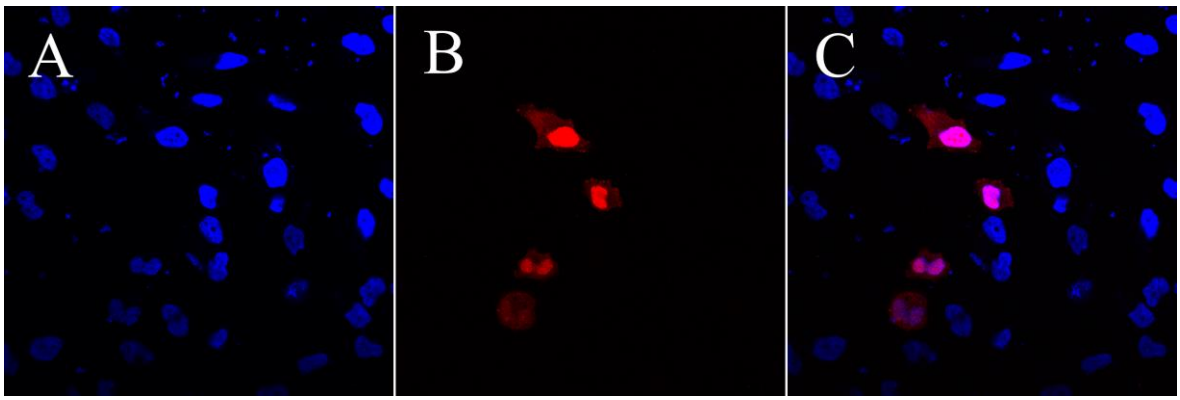

Figure 3. T7 promoter efficiency in induced T7 polymerase-expressing Hela cells. (A) DAPI, (B) mCherry and (C) merge. The cells were transfected with a pUC18-T7-mCherry plasmid and fixed after ca. 30 hours. Cell nuclei were labelled with DAPI before confocal fluorescence microscopy.

3.2 RNA probe 1 does not significantly increase eIF2 or PKR phosphorylation in the presence of EV1 genomes

A new method of using *in vitro* transcribed RNA probes was adopted due to low number of Hela cells actively expressing T7 polymerase (Figure 3). The following experiments were conducted by transfecting an *in vitro*-transcribed RNA probe with no human genome off-targets (T7p_E1F_1) to A549 cells. Cellular response to EV1 infection in the form of both eIF2 and PKR phosphorylation was monitored at various time points over 6 hours. The level of eIF2α phosphorylation was quite low in general when compared to the levels observed during uninhibited six-hour EV1 infection (Figure 4 A). While untreated A549 cells and those treated with only transfection reagents did not produce much background, the introduction of cycloheximide or the probe increased eIF2α phosphorylation almost as much as exposing them to the probe and EV1 particles (Figure 4). On average, only timepoints 3 and 6 hours p.i. rose above the probe control with no virus infection (Figure 4 B). However, neither of these timepoints was significant (Table 1).

PKR phosphorylation was virtually undetected in untreated A549 cells or the ones treated with cycloheximide, both cycloheximide and EV1 particles, or transfection reagents (Figure 4). Conversely, introducing the probe to cycloheximide-treated A549 cells increased the level of PKR phosphorylation. However, the levels observed in cells lysed from 2 to 3.5 hours p.i. were generally higher than those of probe control which suggests that the level of phosphorylation is the highest during these times (Figure 4). Nonetheless, the variation between replicates was high and two-tailed Welch's t-test failed to support this observation with P values above 0.05 (Table 1).

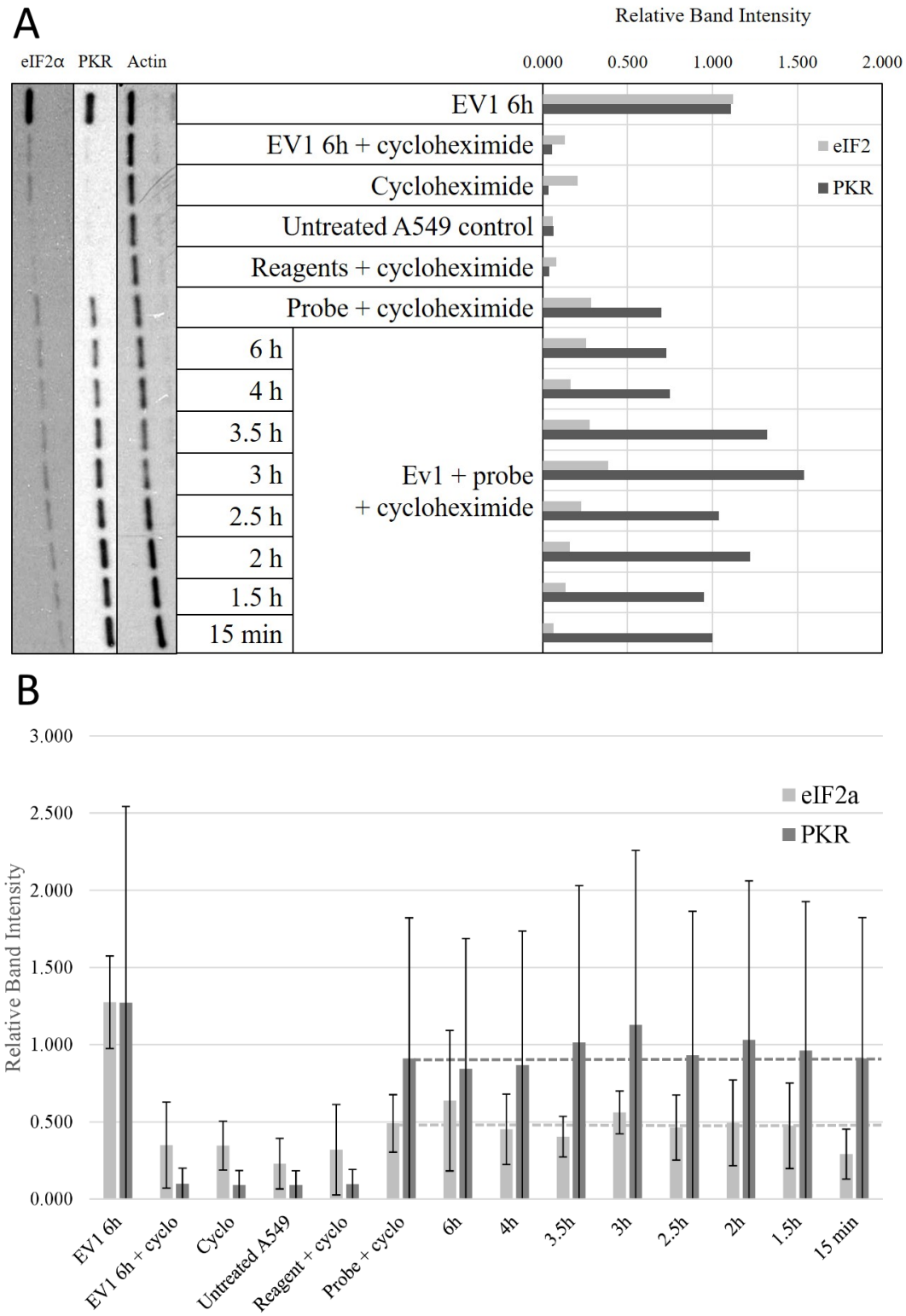

Figure 4. Increase in eIF2α and PKR phosphorylation in one RNA probe system. (A): Representative Western blot results and their quantification: A549 cells transfected with one RNA probe and infected with EV1 for different times. A549 cells were infected with uninhibited EV1 as a positive control for eIF2α, PKR, and actin signal. (B): Average Western blot quantification results as a mean of three experiments with standard deviation. Welch's two-tailed t-test did not indicate that increase in phosphorylation at any timepoint p.i.was significant (Table 1).

Table 1. Increase in eIF2α and PKR in one RNA probe system. Unpaired, two-tailed Welch's T-test of transfected and infected cells controlled with transfected but noninfected cells.

	P value	
Time Post-infection	eIF2a	PKR
6 h	0.70149	0.70545
4 h	0.86210	0.81716
3.5 h	0.62155	0.66916
3 h	0.68599	0.45791
2.5 h	0.89881	0.89748
2 h	0.98898	0.52998
1.5 h	0.95001	0.76906
15 min	0.31725	0.99709

3.3 RNA egress most likely to occur approximately 3 hours post infection

All three RNA probes, homologous to different loci of EV1 genome, were transfected simultaneously into A549 cells that were then infected with EV1. This procedure was theorised to produce more dsRNA and therefore more material for PKR activation by phosphorylation leading to easier detection of changes in phosphorylation status. These experiments revealed a trend dissimilar to the one observed during the transfection of a single probe: earlier timepoints (2 hours p.i. or fewer) were more likely to indicate extremely high levels of PKR phosphorylation (Figure 5). From 2.5 to 3.5 hours p.i., these levels declined, while remaining higher than probe transfection control or even 6-hour uninhibited infection. The levels remained at probe control levels at 4 and 6 hours p.i. Even though cellular background was generally low, the introduction of cycloheximide, transfection reagents or the probes caused some increase in phosphorylation levels (Figure 5).

Interestingly, two-tailed Welch's t-test revealed that the levels of phosphorylation observed at 2.5 to 3.5 hours p.i. were significant (p-values for 2.5, 3, and 3.5 hours were 0.0007, 0.038 and 0.004, respectively) indicating, that the phosphorylation at

these timepoints is more likely to be caused by the introduction of both the probe and the viral genome (Table 2, Figure 5,). Other timepoints did not indicate such a strong correlation as their P values were higher than 0.05.

Table 2. Increase in PKR phosphorylation in three RNA probe system. Unpaired, two-tailed Welch's T-test of transfected and infected cells controlled with transfected but noninfected cells (* significant at P<0.05, ** significant at P<0.01, and *** significant at P<0.001).

	P value
Time	PKR
6h	0.38507
4h	0.81580
3.5h	0.00074 ***
3h	0.03770 *
2.5h	0.00385 **
2h	0.14827
1.5h	0.10016
45 min	0.17529

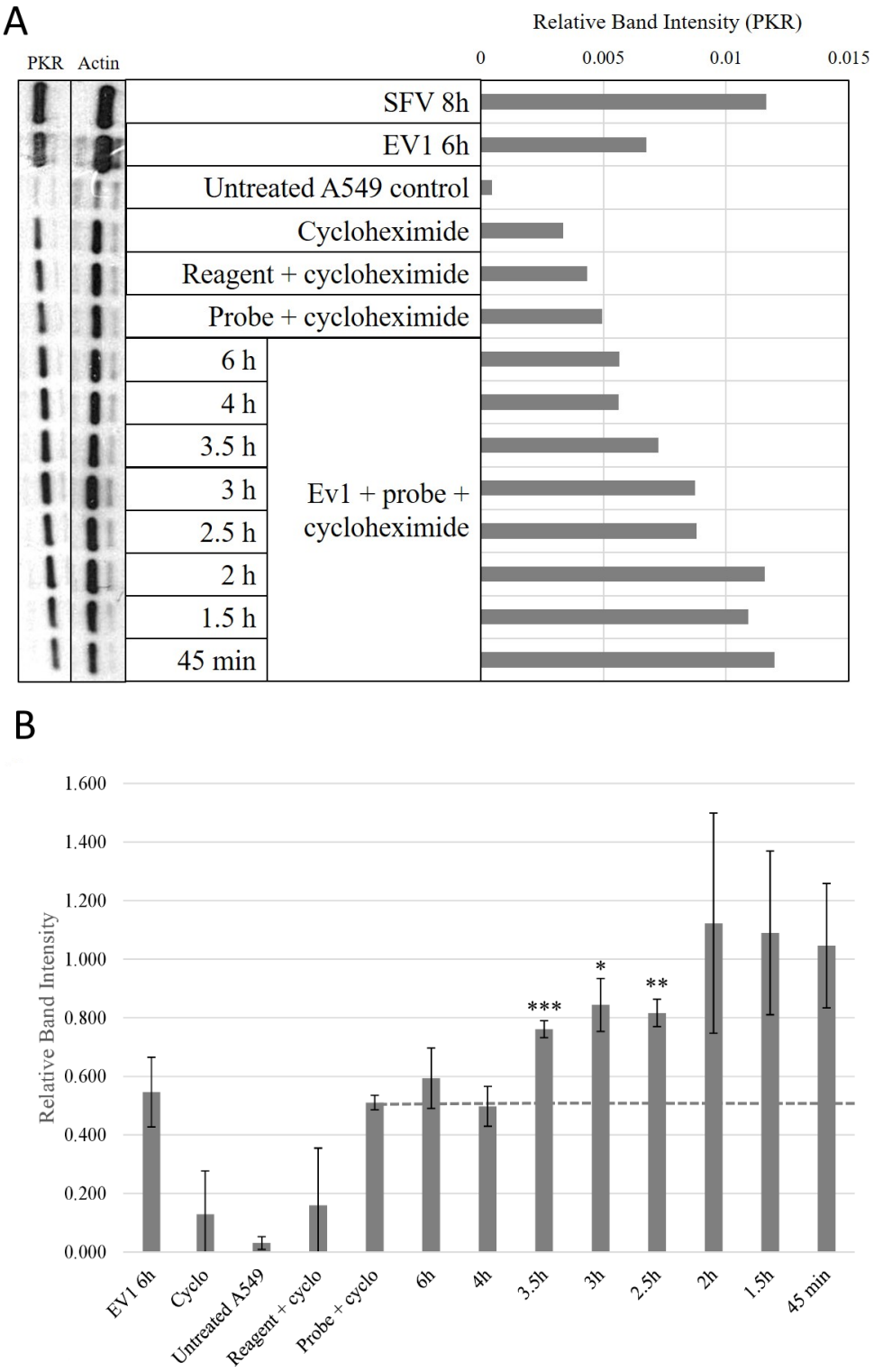

Figure 5. Three Probe System. (A) Representative Western blot results and consequent western blot quantification of A549 cells transfected with three probes and infected with EV1 for different times. Semliki forest virus (SFV) and EV1-infected cell lysates were used as positive controls for PKR and actin signal (B) Average quantification results as a mean of three experiments with standard deviation. The most promising significant times p.i. were 2.5, 3, and 3.5 hours p.i. which suggests that endosomal egress of the viral genome occurs during this time (* significant at $P<0.05$, ** significant at $P<0.01$, and *** significant at $P<0.001$).

4 DISCUSSION

In order to successfully infect a cell, EV1 needs to deliver its genome through the membrane of the multivesicular bodies in which it is internalised. The exact timing and mechanism of this step on the infection timeline are yet to be established. Here we studied whether endosomal egress can be detected by inducing the activation of an antiviral signalling protein, PKR. This process involved transfecting single-stranded RNA probes, complementary to EV1 genome, during EV1 infection into cells with impaired translation. If improved, this assay may help elucidate the mechanism of membrane poration and could be used to screen for antiviral drugs that block the membrane-crossing step.

4.1 Time of endosomal egress

The highest levels of phosphorylation were observed during early timepoints of the three-probe transfection system (Figure 5 B). It is possible that egress occurs before 1 hours p.i. since the bulk of uncoating events occur during this time (Siljamäki et al., 2013). However, endosomal compartment permeabilization is only observed 1−3 hours p.i. and the first signs of active RNA replication appear after 3 hours making egress at such early timepoints unlikely (Upla et al., 2008, Soonsawad et al., 2014). A similar timeline of infection has been established for a closely related enterovirus, Coxsackievirus A9, which further suggests that phosphorylation at these early timepoints was unrelated to probe hybridisation to EV1 genomes (Huttunen et al., 2014). This similarity was reflected by the fact that the phosphorylation levels during these timepoints were not significant (Table 1, Table 2). It is more likely that the elevated levels of phosphorylation during these early timepoints are related to other aspects of the treatment that elicited a stress response in the cells.

PKR has been associated with various stress response pathways, including those related to interferon responses (Patel and Sen, 1998): the presence of viral particles alone may activate PKR. Moreover, factors such as translational inhibition and temperature changes may induce the translation of certain transposable ALU elements in the human genome leading to PKR activation (Chu et al., 1998). This ALU translation-mediated PKR activation may contribute to some of the high background phosphorylation in probe-transfected controls, though this was not reflected by the levels of phosphorylation in cells infected by EV1 in the presence of cycloheximide at 6 hours p.i. which remained low (Figure 4, Figure 5).

One could theorise that subjecting cells to one kind of stress could predispose the cellular signalling machinery to responding more excessively to another. For instance, introducing a translational inhibitor or adding viral particles to the medium might not induce as much phosphorylation alone but could cause a higher degree of cellular response together. This effect amplification would be particularly noticeable in pathways that share overlapping amplification cascade hub elements such as PKR. Curiously, such a strong response within 2 hours p.i. was not observed when the cells were transfected with just one probe despite similar treatment (Figure 4, Figure 5). The absence of such elevated phosphorylation levels at early time points when transfected with one probe and the increase in phosphorylation in transfected but noninfected cells suggest that these cells are responding to dsRNA comprised of cellular mRNA and RNA probes 2 and 3. PKR activation caused by this duplexing may be the most likely explanation for the increased phosphorylation at these early timepoints as probes 2 and 3 were known to have some homology with the human transcriptome.

The most significant timepoints were 2.5, 3, and 3.5 hours p.i. (p-values were 0.0007, 0.038 and 0.004, respectively. Table 2) of the one-probe system and the high levels of phosphorylation during these times fit the established canonical timeline of infection described above. Elevated phosphorylation levels may have been

observed over this long time span since not all viruses release their genome at once, especially since the infection was not synchronised. The three timepoints above could potentially be used in antiviral drug screens that attempt to determine whether the drug affects viruses' ability to cross the endosomal membrane.

4. Improvements

The level of T7 polymerase expression in the T7 competent Hela cells used in the DNA probe transfection system may have been low and the efficacy of probe transcription in these cells may have been lower than desirable, as indicated by poor mCherry expression levels (Figure 3). Taking these facts into account, DNA probes were replaced with *in vitro* transcribed RNA probes. During the tests conducted with single-probe transfection systems, it became clear that either the increase in eIF2 phosphorylation was below accurate detection limit or that the antibody was working in an unpredictable way. This unpredictability could be seen occasionally as even bands across all eIF2α samples (Figure 4 A). As a result, the eIF2α antibody was not used in the three-probe transfection system.

The underlying issue with both 1 RNA probe and 3 RNA probe systems was the amount of variation between replicates: the standard deviations displayed in Figure 4 and Figure 5 are high. This may be a result of the Western blot quantification method which introduces many variables into the equation. Factors such as film exposure time and film quality affect the assay in unpredictable ways. The method may benefit from switching to a more easily quantifiable analysis method such as ELISA which may help eliminate some of the variation observed.

As partially evidenced by poor mCherry expression in Hela T7 cells, transfection efficiency may have been a major contributing factor to inconsistent results. Lipid-based transfection, while easy, quick, nontoxic, and highly effective, can result in varying levels of efficiency depending on the properties of cell lines in question and

the ratio of nucleic acid to lipid (Birchall et al., 1999). Moreover, transient transfection of both DNA and RNA is, by definition, temporary, and thus fickler. Many small RNA oligonucleotides, such as siRNAs, are usually diluted relatively rapidly (within days) in actively dividing cells (Bartlett and Davis, 2006): probe concentrations may vary drastically over time and between treatments.

In the light of the above, the probe delivery system used could be improved by genetically modifying a cell line with an insert containing the desired homology sequence. Viral vectors have successfully been used as tools for permanent genetic modification for decades due to their natural ability to enter host cells and deliver genetic material contained in their capsids. This approach has seen numerous applications such as corrective cancer therapies (Mancheño-Corvo and Martín-Duque, 2006).

An alternative, more visual approach could involve microscopy and Cas-proteins. Clustered regularly interspaced palindromic repeats (CRISPR) and CRISPR-associated proteins (Cas), collectively known as CRISPR/Cas, are components of a system of bacterial adaptive immunity (Barrangou et al., 2007). CRISPR sequences are composed of nucleic acid sequences copied from invading bacteriophages and integrated into the bacterial genome (Brouns et al., 2008). These sequences are then transcribed into short strands of RNA, known as guide RNA and bound to certain Cas proteins. These guide RNA-Cas complexes can locate sequences homologous to the guide RNA which is then cut at a certain position by the Cas proteins' catalytic domains (Garneau et al., 2010). This mechanism of cutting was rapidly exploited as an extremely precise genome editing tool and it remains one of the most effective methods on the market.

However, Cas proteins are not only useful as DNA and RNA-cutting tools: they can be harnessed to locate specific sequences in living cells as DNA or RNA-binding proteins. For this end, certain variants of deactivated Cas proteins (dCas) with

defects in their catalytic domains were developed. When it comes to the detection of enteroviral RNA genomes, dCas13a is of particular interest: it is a deactivated Cas protein with an affinity for single-stranded RNA (Abudayyeh et al., 2018). This protein was successfully used in imaging mRNA localisation by Abudayyeh et al. (2018) when equipped with recombinant fluorescent tags.

This method of visualisation has been used quite stunningly in what was dubbed "chromosome painting", essentially Cas-mediated fluorescent *in situ* hybridisation in living cells (Qin et al., 2017). In these experiments, the targets were mostly repetitive genomic regions and gene loci of considerable length, whereas an enteroviral genome is only a few thousand base pairs long and characterized by compact, non-repetitive sequences. The lack of repetitive sequences in the viral genome means that a few fluorescent tags on viral genomes might not be enough for detection: each genome would need to be equipped with dozens, if not hundreds, of gRNA-Cas complexes. Accurate detection would require introducing more gRNAs into the cell simultaneously, increasing the chance of off-targets in host genome and mRNA as well as the possibility of eliciting stress responses. Nevertheless, successful labelling of non-repetitive sequences with only four unique gRNAs has been reported (Qin et al., 2017) with an approach that utilises extended MS2 capsid protein-binding motif RNA tags in the gRNA and MS2 capsid protein-tagged fluorochromes. Due to the low amount of fluorescence, this method does require advanced microscopy techniques and equipment, but it was stated by Quin et al. (2017) that more conventional microscopy methods can be used with just eight unique gRNAs.

4 CONCLUSIONS

When detected by phosphorylation-specific antibodies, PKR T446 phosphorylation may indicate EV1 genome release from endosomes into the cytoplasm. Most of this egress is likely to occur ca. 2.5−3.5 hours p.i. in A549 cells, as expected based on what is known about the timing of internalisation, uncoating, and translation. The variation between replicates made the analysis of the data difficult so the main focus of future development needs to be its reduction. In order to establish whether this timeline is universal in the genus Enterovirus, the methods should be replicated using various enteroviruses, such as the type species coxackievirus B3 or poliovirus. Further studies in which several cell lines are used may also shed light on the variation in the speed at which the infection of various enteroviruses progresses in different hosts and host cells.

If improved, the assay developed here may also be used to screen for antiviral drugs that target the pre-cytoplasmic steps of infection. The absence of increased PKR T446 phosphorylation would indicate that the drug blocked the infection before it could advance past the endosome. Establishing when the egress occurs may also help capture the very moment and proteins involved in the release from endosomes. Further development and research are needed to improve this method so that it can be used as a reliable tool in the search for new antiviral molecules.

ACKNOWLEDGEMENTS

I would like to thank my supervisors, Mira Laajala and Dr. Varpu Marjomäki whose invaluable advice and guidance allowed me to perform to the best of my abilities. I am also grateful for the counsel of Dr. Giuseppe Balistreri (University of Helsinki) who also graciously supplied us with T7 Hela cells and SFV-infected Hela lysate. His designs and ideas truly brought this project into life. I would also like to express my gratitude towards Dr. Sami Oikarinen (University of Tampere) who designed the probes used in this study, Dr. Kostya Konstantin (DNA dream lab, University of Helsinki) for synthesising these probes, and Dr. Tero Ahola (Univeristy of Helsinki) for providing us an aliquot of pUC18-mCherry plasmid. The work would not have been possible without these vital materials. Last but not least, I thank everyone else at the Varpu Marjomäki group: Paula Turkki, Visa Ruokolainen, Dhanik Reshamwala, Tino Kantoluoto, and Niko Kangasniem for creating a supportive and dynamic working environment.

REFERENCES

Abudayyeh O.O., Gootenberg J.S., Essletzbichler P., Han S., Joung J., Belanto J.J., Verdine V., Cox D.B.T., Kellner M.J., Regev A., Lander E.S., Voytas D.F., Ting A.Y. & Zhang F. 2017. RNA targeting with CRISPR-Cas13. *Nature* 550: 280-284.

Back S.H., Kim Y.K., Kim W.J., Cho S., Oh H.R., Kim J. & Jang S.K. 2002. Translation of polioviral mRNA is inhibited by cleavage of polypyrimidine tract-binding proteins executed by polioviral 3C(pro). *J Virol* 76: 2529-2542.

Barrangou R., Fremaux C., Deveau H., Richards M., Boyaval P., Moineau S., Romero D.A. & Horvath P. 2007. CRISPR provides acquired resistance against viruses in prokaryotes. *Science* 315: 1709-1712.

Bartlett D.W. & Davis M.E. 2006. 705. A Practical Approach to siRNA-Based Treatment Design Using Bioluminescent Imaging and Mathematical Modeling. *Molecular Therapy* 13: S273, doi:10.1016/j.ymthe.2006.08.784.

Basavappa R., Syed R., Flore O., Icenogle J.P., Filman D.J. & Hogle J.M. 1994. Role and mechanism of the maturation cleavage of VP0 in poliovirus assembly: Structure of the empty capsid assembly intermediate at 2.9 Å resolution. *Protein science : a publication of the Protein Society* 3: 1651-1669.

Belov G.A. & Sztul E. 2014. Rewiring of cellular membrane homeostasis by picornaviruses. *J Virol* 88: 9478-9489.

Belov G.A., Nair V., Hansen B.T., Hoyt F.H., Fischer E.R. & Ehrenfeld E. 2012. Complex dynamic development of poliovirus membranous replication complexes. *J Virol* 86: 302-312.

Bergelson J.M., Shepley M.P., Chan B.M., Hemler M.E. & Finberg R.W. 1992. Identification of the integrin VLA-2 as a receptor for echovirus 1. *Science* 255: 1718-1720.

Birchall J.C., Kellaway I.W. & Mills S.N. 1999. Physico-chemical characterisation and transfection efficiency of lipid-based gene delivery complexes. *Int J Pharm* 183: 195-207.

Bostina M., Levy H., Filman D.J. & Hogle J.M. 2011. Poliovirus RNA is released from the capsid near a twofold symmetry axis. *J Virol* 85: 776-783.

Brouns S.J.J., Jore M.M., Lundgren M., Westra E.R., Slijkhuis R.J.H., Snijders A.P.L., Dickman M.J., Makarova K.S., Koonin E.V. & van der Oost J. 2008. Small CRISPR RNAs guide antiviral defense in prokaryotes. *Science* 321: 960-964.

Butan C., Filman D.J. & Hogle J.M. 2014. Cryo-electron microscopy reconstruction shows poliovirus 135S particles poised for membrane interaction and RNA release. *J Virol* 88: 1758-1770.

Chen Y., Du W., Hagemeijer M.C., Takvorian P.M., Pau C., Cali A., Brantner C.A., Stempinski E.S., Connelly P.S., Ma H., Jiang P., Wimmer E., Altan-Bonnet G. & Altan-Bonnet N. 2015. Phosphatidylserine vesicles enable efficient en bloc transmission of enteroviruses. *Cell* 160: 619-630.

Chu W.M., Ballard R., Carpick B.W., Williams B.R. & Schmid C.W. 1998. Potential Alu function: regulation of the activity of double-stranded RNA-activated kinase PKR. *Mol Cell Biol* 18: 58-68.

Cole J.L. 2007. Activation of PKR: an open and shut case? *Trends Biochem Sci* 32: 57-62.

Cuddihy A.R., Li S., Tam N.W., Wong A.H., Taya Y., Abraham N., Bell J.C. & Koromilas A.E. 1999. Double-stranded-RNA-activated protein kinase PKR enhances transcriptional activation by tumor suppressor p53. *Mol Cell Biol* 19: 2475-2484.

Danthi P., Tosteson M., Li Q. & Chow M. 2003. Genome delivery and ion channel properties are altered in VP4 mutants of poliovirus. *J Virol* 77: 5266-5274.

Deb A., Zamanian-Daryoush M., Xu Z., Kadereit S. & Williams B.R. 2001. Protein kinase PKR is required for platelet-derived growth factor signaling of c-fos gene expression via Erks and Stat3. *EMBO J* 20: 2487-2496.

Dey M., Cao C., Dar A.C., Tamura T., Ozato K., Sicheri F. & Dever T.E. 2005. Mechanistic link between PKR dimerization, autophosphorylation, and eIF2alpha substrate recognition. *Cell* 122: 901-913.

Erickson F.L., Harding L.D., Dorris D.R. & Hannig E.M. 1997. Functional analysis of homologs of translation initiation factor 2gamma in yeast. *Mol Gen Genet* 253: 711-719.

Filman D.J., Syed R., Chow M., Macadam A.J., Minor P.D. & Hogle J.M. 1989. Structural factors that control conformational transitions and serotype specificity in type 3 poliovirus. *The EMBO Journal* 8: 1567-1579.

Flanegan J.B. & Baltimore D. 1977. Poliovirus-specific primer-dependent RNA polymerase able to copy poly(A). *Proc Natl Acad Sci U S A* 74: 3677-3680.

Garneau J.E., Dupuis M., Villion M., Romero D.A., Barrangou R., Boyaval P., Fremaux C., Horvath P., Magadán A.H. & Moineau S. 2010. The CRISPR/Cas bacterial immune system cleaves bacteriophage and plasmid DNA. *Nature* 468: 67-71.

Gaspar N.J., Kinzy T.G., Scherer B.J., Hümbelin M., Hershey J.W. & Merrick W.C. 1994. Translation initiation factor eIF-2. Cloning and expression of the human cDNA encoding the gamma-subunit. *J Biol Chem* 269: 3415-3422.

Groppelli E., Levy H.C., Sun E., Strauss M., Nicol C., Gold S., Zhuang X., Tuthill T.J., Hogle J.M. & Rowlands D.J. 2017. Picornavirus RNA is protected from cleavage by ribonuclease during virion uncoating and transfer across cellular and model membranes. *PLoS Pathog* 13: e1006197, doi:10.1371/journal.ppat.1006197.

Hershey J.W. 1989. Protein phosphorylation controls translation rates. *The Journal of biological chemistry* 264: 20823.

Hinnebusch A.G. 2014. The scanning mechanism of eukaryotic translation initiation. *Annu Rev Biochem* 83: 779-812.

Hsu N., Ilnytska O., Belov G., Santiana M., Chen Y., Takvorian P.M., Pau C., van der Schaar H., Kaushik-Basu N., Balla T., Cameron C.E., Ehrenfeld E., van Kuppeveld, Frank J. M. & Altan-Bonnet N. 2010. Viral reorganization of the secretory pathway generates distinct organelles for RNA replication. *Cell* 141: 799-811.

Huttunen M., Waris M., Kajander R., Hyypiae T. & Marjomaeki V. 2014. Coxsackievirus A9 Infects Cells via Nonacidic Multivesicular Bodies. *Journal of Virology* 88: 5138-5151.

Huynh T.P., Jancovich J.K., Tripuraneni L., Heck M.C., Langland J.O. & Jacobs B.L. 2017. Characterization of a PKR inhibitor from the pathogenic ranavirus, Ambystoma tigrinum virus, using a heterologous vaccinia virus system. *Virology* 511: 290-299.

Ilnytska O., Santiana M., Hsu N., Du W., Chen Y., Viktorova E.G., Belov G., Brinker A., Storch J., Moore C., Dixon J.L. & Altan-Bonnet N. 2013. Enteroviruses harness the cellular endocytic machinery to remodel the host cell cholesterol landscape for effective viral replication. *Cell Host Microbe* 14: 281-293.

Jang S.K., Pestova T.V., Hellen C.U., Witherell G.W. & Wimmer E. 1990. Cap-independent translation of picornavirus RNAs: structure and function of the internal ribosomal entry site. *Enzyme* 44: 292-309.

Karjalainen M., Rintanen N., Lehkonen M., Kallio K., Mäki A., Hellström K., Siljamäki V., Upla P. & Marjomäki V. 2011. Echovirus 1 infection depends on biogenesis of novel multivesicular bodies. *Cell Microbiol* 13: 1975-1995.

Karjalainen M., Kakkonen E., Upla P., Paloranta H., Kankaanpää P., Liberali P., Renkema G.H., Hyypiä T., Heino J. & Marjomäki V. 2008. A Raft-derived, Pak1-regulated entry participates in alpha2beta1 integrin-dependent sorting to caveosomes. *Mol Biol Cell* 19: 2857-2869.

Keller C., Mellouk N., Danckaert A., Simeone R., Brosch R., Enninga J. & Bobard A. 2013. Single cell measurements of vacuolar rupture caused by intracellular pathogens. *J Vis Exp* : e50116, doi:10.3791/50116.

Kimball S.R. 1999. Eukaryotic initiation factor eIF2. *International Journal of Biochemistry and Cell Biology* 31: 25-29.

Krieger S.E., Kim C., Zhang L., Marjomaki V. & Bergelson J.M. 2013. Echovirus 1 entry into polarized Caco-2 cells depends on dynamin, cholesterol, and cellular factors associated with macropinocytosis. *J Virol* 87: 8884-8895.

Laitinen O.H., Honkanen H., Pakkanen O., Oikarinen S., Hankaniemi M.M., Huhtala H., Ruokoranta T., Lecouturier V., André P., Harju R., Virtanen S.M., Lehtonen J., Almond J.W., Simell T., Simell O., Ilonen J., Veijola R., Knip M. & Hyöty H. 2014. Coxsackievirus B1 is associated with induction of β-cell autoimmunity that portends type 1 diabetes. *Diabetes* 63: 446-455.

Lee J.H., Park E.J., Kim O.S., Kim H.Y., Joe E. & Jou I. 2005. Double-stranded RNA-activated protein kinase is required for the LPS-induced activation of STAT1 inflammatory signaling in rat brain glial cells. *Glia* 50: 66-79.

Lemaire P.A., Tessmer I., Craig R., Erie D.A. & Cole J.L. 2006. Unactivated PKR exists in an open conformation capable of binding nucleotides. *Biochemistry* 45: 9074-9084.

Mancheño-Corvo P. & Martín-Duque P. 2006. Viral gene therapy. *Clin Transl Oncol* 8: 858-867.

Marjomäki V., Turkki P. & Huttunen M. 2015. Infectious Entry Pathway of Enterovirus B Species. *Viruses* 7: 6387-6399.

Marjomäki V., Pietiäinen V., Matilainen H., Upla P., Ivaska J., Nissinen L., Reunanen H., Huttunen P., Hyypiä T. & Heino J. 2002. Internalization of echovirus 1 in caveolae. *J Virol* 76: 1856-1865.

Meurs E., Chong K., Galabru J., Thomas N.S., Kerr I.M., Williams B.R. & Hovanessian A.G. 1990. Molecular cloning and characterization of the human double-stranded RNA-activated protein kinase induced by interferon. *Cell* 62: 379-390.

Myllynen M., Kazmertsuk A. & Marjomäki V. 2016. A Novel Open and Infectious Form of Echovirus 1. *J Virol* 90: 6759-6770.

Palmenberg A.C. 1990. Proteolytic processing of picornaviral polyprotein. *Annu Rev Microbiol* 44: 603-623.

Panjwani A., Strauss M., Gold S., Wenham H., Jackson T., Chou J.J., Rowlands D.J., Stonehouse N.J., Hogle J.M. & Tuthill T.J. 2014. Capsid protein VP4 of human rhinovirus induces membrane permeability by the formation of a size-selective multimeric pore. *PLoS Pathog* 10: e1004294, doi: 10.1371/journal.ppat.1004294.

Patel R.C. & Sen G.C. 1998. PACT, a protein activator of the interferon-induced protein kinase, PKR. *EMBO J* 17: 4379-4390.

Paul A.V., van Boom J.H., Filippov D. & Wimmer E. 1998. Protein-primed RNA synthesis by purified poliovirus RNA polymerase. *Nature* 393: 280-284.

Paula Upla, Varpu Marjomäki, Liisa Nissinen, Camilla Nylund, Matti Waris, Timo Hyypiä & Jyrki Heino. 2008. Calpain 1 and 2 Are Required for RNA Replication of Echovirus 1. *Journal of Virology* 82: 1581-1590.

Peiwu Qin, Mahmut Parlak, Cem Kuscu, Jigar Bandaria, Mustafa Mir, Karol Szlachta, Ritambhara Singh, Xavier Darzacq, Ahmet Yildiz & Mazhar Adli. 2017. Live cell imaging of low- and non-repetitive chromosome loci using CRISPR-Cas9. *Nature Communications* 8: 14725, doi: 10.1038/ncomms14725.

Pietiäinen V., Marjomäki V., Upla P., Pelkmans L., Helenius A. & Hyypiä T. 2004. Echovirus 1 endocytosis into caveosomes requires lipid rafts, dynamin II, and signaling events. *Mol Biol Cell* 15: 4911-4925.

Rintanen N., Karjalainen M., Alanko J., Paavolainen L., Mäki A., Nissinen L., Lehkonen M., Kallio K., Cheng R.H., Upla P., Ivaska J. & Marjomäki V. 2012. Calpains promote α2β1 integrin turnover in nonrecycling integrin pathway. *Mol Biol Cell* 23: 448-463.

Robinson S.M., Tsueng G., Sin J., Mangale V., Rahawi S., McIntyre L.L., Williams W., Kha N., Cruz C., Hancock B.M., Nguyen D.P., Sayen M.R., Hilton B.J., Doran K.S., Segall A.M., Wolkowicz R., Cornell C.T., Whitton J.L., Gottlieb R.A. & Feuer R. 2014. Coxsackievirus B exits the host cell in shed microvesicles displaying autophagosomal markers. *PLoS Pathog* 10: e1004045, doi:10.1371/journal.ppat.1004045.

Roivainen M., Alfthan G., Jousilahti P., Kimpimäki M., Hovi T. & Tuomilehto J. 1998. Enterovirus infections as a possible risk factor for myocardial infarction. *Circulation* 98: 2534-2537.

Romano P.R., Garcia-Barrio M.T., Zhang X., Wang Q., Taylor D.R., Zhang F., Herring C., Mathews M.B., Qin J. & Hinnebusch A.G. 1998. Autophosphorylation in the activation loop is required for full kinase activity in vivo of human and yeast eukaryotic initiation factor 2alpha kinases PKR and GCN2. *Mol Cell Biol* 18: 2282-2297.

Rotbart H.A., Brennan P.J., Fife K.H., Romero J.R., Griffin J.A., McKinlay M.A. & Hayden F.G. 1998. Enterovirus Meningitis in Adults. *Clinical Infectious Diseases* 27: 896-898.

Scheuner D., Patel R., Wang F., Lee K., Kumar K., Wu J., Nilsson A., Karin M. & Kaufman R.J. 2006. Double-stranded RNA-dependent protein kinase phosphorylation of the alpha-subunit of eukaryotic translation initiation factor 2 mediates apoptosis. *J Biol Chem* 281: 21458-21468.

Schindelin J., Arganda-Carreras I., Frise E., Kaynig V., Longair M., Pietzsch T., Preibisch S., Rueden C., Saalfeld S., Schmid B., Tinevez J., White D.J., Hartenstein V., Eliceiri K., Tomancak P. & Cardona A. 2012. Fiji: an open-source platform for biological-image analysis. *Nature Methods* 9: 676-682.

Siljamäki E., Rintanen N., Kirsi M., Upla P., Wang W., Karjalainen M., Ikonen E. & Marjomäki V. 2013. Cholesterol dependence of collagen and echovirus 1 trafficking along the novel α2β1 integrin internalization pathway. *PLoS ONE* 8: e55465, doi:10.1371/journal.pone.0055465.

Simeone R., Bobard A., Lippmann J., Bitter W., Majlessi L., Brosch R. & Enninga J. 2012. Phagosomal rupture by Mycobacterium tuberculosis results in toxicity and host cell death. *PLoS Pathog* 8: e1002507, doi:10.1371/journal.ppat.1002507.

Smyth M., Pettitt T., Symonds A. & Martin J. 2003. Identification of the pocket factors in a picornavirus. *Arch Virol* 148: 1225-1233.

Soonsawad P., Paavolainen L., Upla P., Weerachatyanukul W., Rintanen N., Espinoza J., McNerney G., Marjomäki V. & Cheng R.H. 2014. Permeability changes of integrin-containing multivesicular structures triggered by picornavirus entry. *PLoS ONE* 9: e108948, doi:10.1371/journal.pone.0108948.

Staring J., von Castelmur E., Blomen V.A., van den Hengel, Lisa G., Brockmann M., Baggen J., Thibaut H.J., Nieuwenhuis J., Janssen H., van Kuppeveld, Frank J. M., Perrakis A., Carette J.E. & Brummelkamp T.R. 2017. PLA2G16 represents a switch between entry and clearance of Picornaviridae. *Nature* 541: 412-416.

Su Q., Wang S., Baltzis D., Qu L., Wong A.H. & Koromilas A.E. 2006. Tyrosine phosphorylation acts as a molecular switch to full-scale activation of the eIF2alpha RNA-dependent protein kinase. *Proc Natl Acad Sci U S A* 103: 63-68.

Takeuchi O. & Akira S. 2009. Innate immunity to virus infection. *Immunol Rev* 227: 75-86.

Tosteson M.T. & Chow M. 1997. Characterization of the ion channels formed by poliovirus in planar lipid membranes. *J Virol* 71: 507-511.

Tuthill T.J., Groppelli E., Hogle J.M. & Rowlands D.J. 2010. Picornaviruses. *Current topics in microbiology and immunology* 343: 43.

van den Heuvel J., Lang V., Richter G., Price N., Peacock L., Proud C. & McCarthy J.E. 1995. The highly acidic C-terminal region of the yeast initiation factor subunit 2 alpha (eIF-2 alpha) contains casein kinase phosphorylation sites and is essential for maintaining normal regulation of GCN4. *Biochim Biophys Acta* 1261: 337-348.

Williams B.R. 1999. PKR; a sentinel kinase for cellular stress. *Oncogene* 18: 6112-6120.

Wimmer E., Hellen C.U. & Cao X. 1993. Genetics of poliovirus. *Annu Rev Genet* 27: 353-436.

Xing L., Huhtala M., Pietiäinen V., Käpylä J., Vuorinen K., Marjomäki V., Heino J., Johnson M.S., Hyypiä T. & Cheng R.H. 2004. Structural and functional analysis of integrin alpha2I domain interaction with echovirus 1. *J Biol Chem* 279: 11632-11638.

Yogo Y. & Wimmer E. 1972. Polyadenylic acid at the 3'-terminus of poliovirus RNA. *Proc Natl Acad Sci U S A* 69: 1877-1882.

APPENDIX 1. OLIGONUCLEOTIDE PROBE SEQUENCES

Corresponding EV1 Farouk strain reference genome sequence positions from 5′ end in brackets. T7 promoter in red.

Probe #1 ″T7p_E1F_1″ (3574-3613):

TAA TAC GAC TCA CTA TAG ACC AAT CCC ACG TGC TTC TTG CAG CCG GAT TTT CTG AAC C

Probe #2 ″T7p_E1F_2″ (939-978):

TAA TAC GAC TCA CTA TAG CCA GCG CTG AAT TCT CCA ACG GTT GAA GAG TGC GGG TAC A

Probe #3 ″T7p_E1F_3″ (3118-3159):

TAA TAC GAC TCA CTA TAG ACG TAA ACA AGC CCA ACC CAG CCG CTA TTA CAA GTG TGG CGC

Designed by Sami Oikarinen PhD, University of Tampere.